Finite element comparative analysis software of a radial flux permanent magnet synchronous motor for electric vehicle drive

R. Abdelmoula abdelmoula.rehab@gmail.com
N. Ben hadj naourez.benhadj@enis.tn
M. Chaieb chaieb_med@yahoo.fr
R.NEJI rafik.neji@enis.rnu.tn

Abstract-- **The choice of finite element (FE) software for motor analysis is an important factor in determining the quality and scope of analysis that can be performed. In this report, a comparative study is presented on two finite element analysis (FEA) softwares to validate a radial flux permanent magnet synchronous motor (RF-PMSM) suitable for electric vehicle (EV) drive. The two softwares presented are FEMM and OPERA. In order to determinate the characteristics requirements, a simple vehicle dynamics model that evaluates vehicle performances was considered. An analytical study and validation of the studied motor has been performed. Results of the FEA simulation were compared with analytical values.**

***Index Terms*-- *finite element analysis, software, FEMM, OPERA, RF-PMM, simulation, electric vehicle*.**

1. NOMENCLATURE

M_v: Vehicle weight with full load.
g: Gravity acceleration.
C_{rr}: Rolling resistance coefficient.
C_x: Aerodynamic drag coefficient.
ρ: The air density.
A_f: Frontal area of the vehicle.
S_b: Vehicle basic speed.
S_v: Vehicle speed.
S_{Max}: Vehicle maximum speed.
γ: acceleration imposed by the driver
α: Incline angle.
σ: A coefficient which depends on the inertia of the rotating masses.
R_{wheel}: Wheel radius.
F_T: Total tractive effort.
F_{Ro}: The rolling friction force.
F_{aero}: The aerodynamics force.
F_a: Force related to the acceleration.
F_G: Force related to the slope.
P_T: Total power supplied on the wheel
R_{wheel}: Radius of the wheel.
K: ratio of mechanical reduction
N_{sph}: Number of turns per phase.
Δt: the discretization in time.
L: Motor length.
D_{So}: Stator outer diameter.
D_{Si}: Stator inner diameter.
D_{Ro}: Rotor outer diameter.
D_{Ri}: Rotor inner diameter.
D_B: *Bore* diameter.
H_{Slot}: Slots height.
H_S: stator yoke thickness.
H_M: Magnet height.
A_{slot}: Slots mean angular width.
A_{tooth}: Principal tooth mean angular width.
$A_{thoothi}$: Inserted tooth mean angular width.
A_p: Pole pitch.
H_M: Permanent Magnet height.
A_M: Permanent Magnet angular width.
e: Air gap.
δ: current density.
N_t: number of stator main teeth.
I_{ph}: Current per phase.
B_a: Magnetic induction in the air gap.
B_r: Remanent induction.
B_s: Magnetic induction in the stator.
T_a: The ambient temperature.
μ_M: relative permeability of magnetic materials.
K_{fu}: Magnet leakage coefficient.
K_r: slot-filling coefficient.
p: number of pole pairs.
M_S: Stator material.
M_R: Rotor material.
M_{PM}: Permanent magnets material.
S_M: Magnet section.
S_{tooth}: main tooth section.
r_{tp}: ratio of number of stator teeth to number of pole pairs.
r_1: Ratio of the magnet angular width by the pole pitch.
r_2: Ratio of the main tooth angular width by the magnet angular width.
r_3: Ratio of the inserted tooth angular width by a main tooth angular width.
Flux : Stator flux amplitude.
EMF: EMF amplitude .
T_S: Starting Torque.
T_{EM} : Electromagnetic torque.
T_T: Total torque applied to the drive shaft
Ω : motor angular speed.

2. INTRODUCTION

With the problems of environmental impacts and the necessity to reduce fuel consumption .EVs have the potential to offer an ideal solution for personal mobility in the future. Permanent magnet synchronous motors (PMSM) are used increasingly in the electrical propulsion due to their high efficiency, small size, high torque density, and reliability [1]. PMSM can be classified into

two main concepts, axial-flux permanent magnet synchronous motor (AF-PMSM) and RF-PMSM. AF-PMSMs are generally used in special applications where large diameter and short stack are required. When, RF-PMSMs are very common and used in various industrial applications.

In this work, a RF-PMSM is used because of their simplicity in fabrication and their low cost.[2].

The rest of this paper is organized as follow: section 3 presents vehicle specification which includes dynamic modeling. Section 4 presents a description of the studied motor and a FE validation by two softwares FEMM and OPERA followed by a comparison of the two used softwares. Section 5 contains the conclusion.

3. VEHICLE SPECIFICATION

A. Vehicle dynamics

A quantitative assessment of variables that characterize the operation of the motor, especially those that appear in the specifications, based on descriptive variables of the system. The total resistance to vehicle motion F_T is the sum of the different components of the mechanical forces acting on the EV for a driving cycle (Fig .1). F_{ro}, F_{aero}, F_a and F_G defined in TABLE I are respectively, the rolling friction force, the aerodynamics force, force related to the acceleration, and the force related to the slope. To model the vehicle transmission system, we supposed that:

- The left and the right vehicle sides are considered symmetry at the level of working contacts and the weight distribution.
- The wheels are considered comparable to full and homogeneous discs.
- The effects of the aerodynamic force in the perpendicular axes of the vehicle are negligible compared to the other components applied in the parallel axis [3].

The total tractive effort can be written as in (1):

$$F_T = F_{Ro} + F_{aero} + F_a + F_G \quad (1)$$

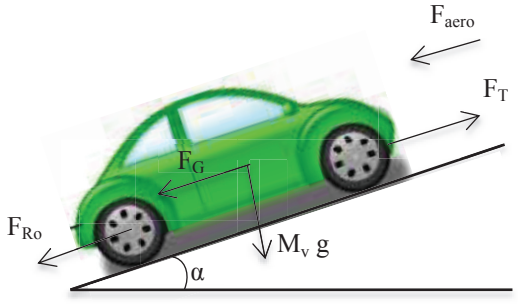

Fig. 1. Forces applied to a vehicle in a slope.

TABLE I

Forces expressions

Symbols	Expression
F_{Ro}	$M_v\ g\ C_{rr}$
F_{aero}	$\frac{1}{2}\rho\ A_f\ C_x\ S_v{}^2$
F_a	$\sigma\ M_v\ \gamma$
F_G	$M_v\ g \sin(\alpha)$

The total torque applied to the drive shaft (2) and the power supplied on the wheel (3) are related to F_T [3]:

$$T_T = F_T\ R_{wheel} \quad (2)$$

$$P_T = S_v . F_T \quad (3)$$

B. EV starting torque

The EV wheels speed begins from a null speed until it attains its basic speed. Over this phase the motor apply a constant starting torque on the wheels. From a null speed up to the maximum vehicle speed the motor exerts a torque, which decreases in proportion to the speed (area of constant power) [4]. Fig. 2 presents the torque in function of the wheels speed.

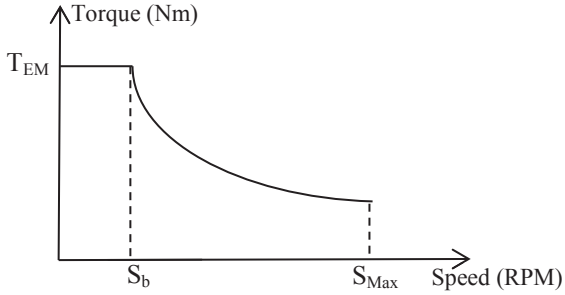

Fig. 2. The torque in function of the wheels speed.

The vehicle parameters are given in TABLE II

TABLE II

Vehicle parameters

Parameters	Values	Units
M_v	1000	Kg
S_b	30	Km/h
S_v	80	Km/h
g	9.81	m/s^2
α	5	%
C_{rr}	0.015	
C_x	0.4	
ρ	1.28	Kg/m^3
γ	1	m/s^2
σ	1,01	
A_f	2	m^2
R_{wheel}	0.26	m
k	6	
t_s	4	s

The electric vehicle must be capable to reach the basic speed during a time t_S. The starting torque of vehicle takes the form in (4) by neglecting the aerodynamic force and the rolling friction force:

$$T_S = R_{wheel}\left(\frac{\sigma M_v R_{wheel} S_b}{t_s} + M_v\, g\, \sin(\alpha)\right) \quad (4)$$

Then the electromagnetic torque is given by the following equation [3]:

$$T_{EM} = \frac{T_S}{k} \quad (5)$$

Vehicle parameters allow calculating the starting torque of the vehicle 669 Nm, and the electromagnetic torque 111.5 Nm.

4. FINITE ELEMENT ANALYSIS: VALIDATION WITH TWO SOFTWARES FEMM AND OPERA

A. Studied motor description

The analysis of the specifications books us to develop a design module based on an analytical model and algebraic equations and to determine all the dimensions defining the machine. The studied machine is a RF-PMSM surface mounted constituted by four pairs of principal pole and six teeth .Between two main teeth, an inserted tooth is added to improve the waveform and reduce the flux leakage (Fig. 3). A concentric winding is used that allows having a reduced space requirement and a better coefficient of winding. Each phase winding is formed by two diametrically opposite coils whose winding is concentrated: the turns of the coil are directly wound around a tooth of the stator. An analytical model is developed in previous research work [3],[5].

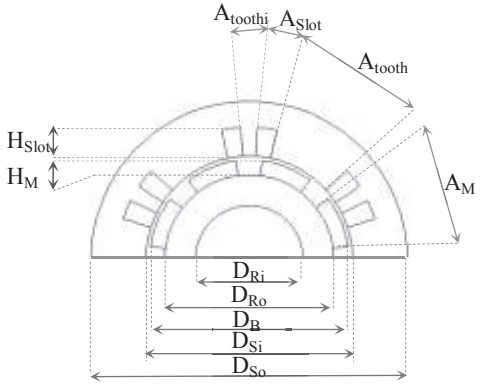

Fig. 3. Half cross section of the studied RFPM motor.

The design of the motor depends on these three ratios:

$$r_1 = \frac{A_M}{A_p} \quad (6)$$

$$r_2 = \frac{A_{tooth}}{A_{PM}} \quad (7)$$

$$r_3 = \frac{A_{toothi}}{A_{tooth}} \quad (8)$$

With

$$A_p = \frac{\pi}{p} \quad (9)$$

In this work, these ratios are fixed and they take respectively the following values: r_1=$\frac{2}{3}$, r_2=$\frac{3}{2}$ et r_3=$\frac{1}{5}$[5].

B. Analytic study

The stator outer diameter D_{So} is calculated from the diameter D_B:

$$D_{So} = D_B + e + 2(H_{slot} + H_s) \quad (10)$$

The angular width of magnet is given by the following expression:

$$A_M = r_1\, A_p \quad (11)$$

The angular width of a main tooth is calculated from the angular width of the magnet and the ratio r_2:

$$A_{tooth} = r_2\, A_M \quad (12)$$

The angular width of an inserted tooth is determined as a function of the angular width of a main tooth and the ratio r_3:

$$A_{toothi} = r_3\, A_{tooth} \quad (13)$$

The section of a main tooth is given by the following expression:

$$S_{tooth} = \frac{D_B+e}{2} L\, A_{tooth} \quad (14)$$

The magnet section is given by (15):

$$S_M = \frac{D_B-e}{2} L\, A_M \quad (15)$$

The angular width of a slot depends on the number of the main teeth; it is given by the following formula:

$$A_{Slot} = \frac{\frac{2\pi}{N_t} - (A_{tooth} + A_{toothi})}{2} \quad (16)$$

The slots height is related to the total number of conductors occupied by the slots and the current density (17):

$$H_{Slot} = \sqrt{\frac{N_{sph} I_{ph}}{\sqrt{2} N_t \delta K_r A_{Slot}} + \left(\frac{D_B+e}{2}\right)^2} - \left(\frac{D_B+e}{2}\right) \quad (17)$$

With

$$N_t = p\, r_{tp} \quad (18)$$

The stator yoke height is given by (19):

$$H_s = \frac{B_a \min(S_{tooth}, S_M)}{2 L B_S} \quad (19)$$

To obtain a magnetic induction in the air gap equal to B_a, the magnet height is given by the following expression:

$$H_M = \frac{\mu_M B_a e}{B_r(T_a) - \frac{B_a}{K_{fu}}} \quad (2)$$

Therefore, the main geometric dimensions of the RF-PMSM motor used in our study are shown in TABLE III.

TABLE III
Dimensions and electromagnetic parameter of the RF-PMSM motor

Parameters	Values	Units
L	250	Mm
μ_M	1.05	H/m
B_r(Ta)	1.175	T
B_a	0.9	T
B_S	0.9	T
T_a	20	°
K_{fu}	0.95	
r_{tp}	1.5	
I_{ph}	63	A
K_r	0.44	
p	4	
N_{sph}	25	spires
D_{So}	127.64	Mm
D_{Si}	102	Mm
H_S	14.15	mm
A_{slot}	8.40	deg
A_{tooth}	29.99	deg
A_{toothi}	35.99	deg
D_{Re}	81.38	mm
D_{Ri}	51	mm
H_M	8.30	mm
A_M	29.99	deg
e	2	mm
M_S	Steel 1010	
M_R	Steel 1010	
M_{PM}	NdFeB	
Flux	0.006	Wb
EMF	226.85	V
T_{EM}	111.5	Nm

C. Simulation results

Finite element analysis method is a process of modeling using mathematical approximation method for simulating real physical system structure. It can be adapted for all kinds of complicated structure, has the distinctive of high precision, and is the effective means of engineering analysis [6]. The modeling by finite elements is both a validation step and an adjustment study. A 2D model of the RF-PMSM motor is made using OPERA2d/RM and FEMM. .The increase of the number of nodes is essential to have a better temporal representation [4]. In OPERA, a rotating machine air gap is a special region which allows the sections of the machine either side of it to rotate. The air gap is constructed from three regions: 2 polygons and a rotating machine air gap region [8].While, in FEEM the air gap is only one region (Fig.4).

After meshing, the magnetic field distribution can be established through the study of the finite element calculation of each node.

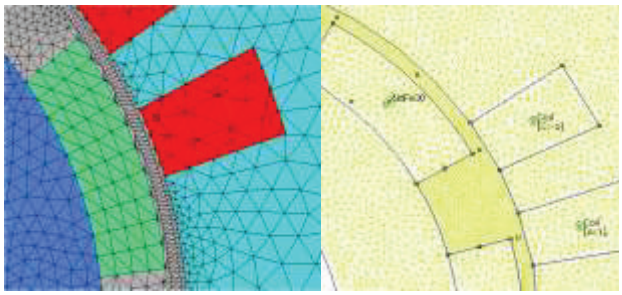

(a) (b)

Fig. 4. Air gap mesh (a) OPERA (b) FEMM.

In the case of no-load, the stator does not create magnetic field. So the no load magnetic field is entirely created by permanent magnets of the rotor. Fig.5 presents the winding captured flux of the machine, for different rotor positions at no load by the two softwares OPERA and FEMM.

Cogging torque is the torque produced at no load condition by the change of the magnetic permeance of the stator teeth and slots over the PMs, and he has no net value [7],[9],[10].Cogging torque curves are almost the same. There is a small decrease in the value of peak value of cogging torque found by OPERA. Fig.6 presents the cogging torque for different rotor position by OPERA and FEMM

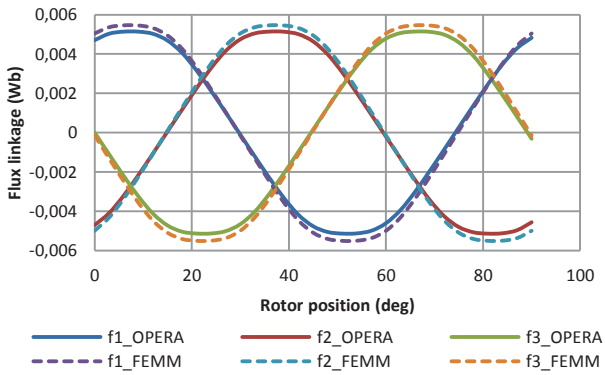

Fig. 5. Flux linkage at no load for different rotor position.

Maximum value of flux found by OPERA and FEMM were respectively 0.0051Wb and 0.0054 Wb which validate analytical value 0.006 Wb.

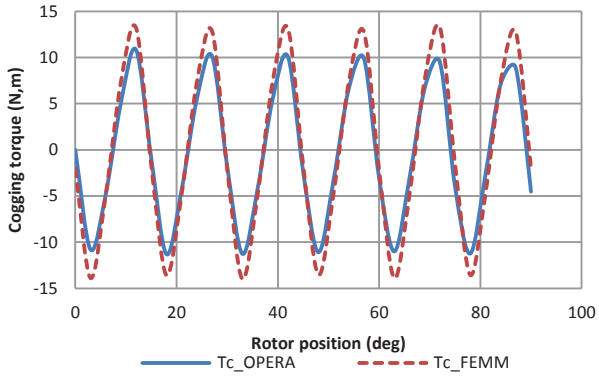

Fig. 6. Cogging torque for different rotor position.

The back-EMF at no load is calculated by deriving the results previously of flux. Back-EMF at time t is determined from the flux values calculated at time t+Δt and t-Δt by the following formula [3].

$$EMF(t) = \frac{\text{Flux}_{t+\Delta t} - \text{Flux}_{t-\Delta t}}{\Delta t}.N_{sph} \quad (21)$$

Back-EMF of the three phases at no load is represented in fig. 7.

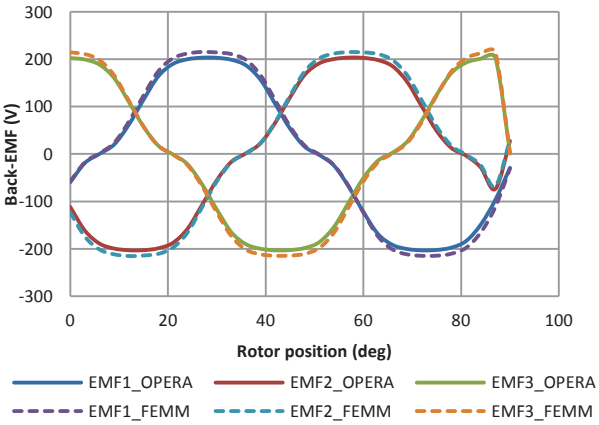

Fig. 7. Back-EMF at no load for different rotor position

Maximum value of Back-EMF found by OPERA and FEMM were respectively 203 V and 214 V which validate analytical value 226V.

Stator winding is feeding with three-phase balanced sinusoidal currents. Electromagnetic torque is calculated simulating load behavior of the motor, for different positions of the rotor. The electromagnetic torque is found by products of the back-EMF by the current as follows [4]:

$$T(t) = \frac{1}{\Omega}\sum EMF(t).i(t) \quad (22)$$

To obtain a maximum torque the current must be in phase with back-EMF. Fig.8 shows the electromagnetic torque calculated.

The average torque value reaches by OPERA and FEMM were respectively 102.6 Nm and 110.1 Nm which validate analytical value 111.5 Nm.

The finite approach validates the analytical calculation.

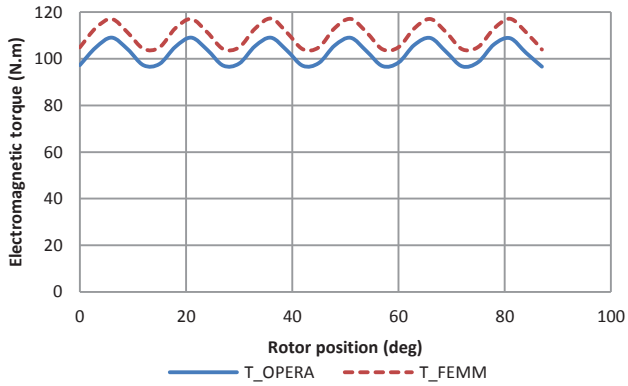

Fig. 8. Electromagnetic torque for different rotor position

D. Comparison of the two software features OPERA and FEMM

The two softwares features are compared in TABLE VI.

TABLE VI
Comparison of the two software features

	FEMM	OPERA
Design	Manual design of work-piece or implement motor control algorithms in octaveFEMM (is a Matlab toolbox that allows for the operation of FEMM)	Work-piece can be designed manual. But commands can also be executed from a script (COMI file) allowing automation of regularly performed tasks and parametrization [8].
Material library	An extensive material library. To define a new materials , preprocessor command set must be written in octaveFEMM	An extensive material library , the program also has the capability of simply defining new materials
Dimension	Module on 2D	Modules for both 2D and 3D
Meshing	Mesh refinement and boundary conditions have to be set manually	Auto-generation of finite element mesh for simulation. Mesh can be refined and modify their form
Solvers	limited solver	many 'solvers' to suit the spectrum of electromagnetic and multiphysics applications
Post-processing results: EMF, cogging torque and electromagnetic torque	Several commands must been written in m file (MATLAB) to get EMF, cogging torque and electromagnetic torque.	OPERA gives directly EMF cogging torque and torque values in Post-processing
Cost	Free	paid

Overall, OPERA has several types of simulations and the user has a good amount of control over the process conditions and gives very quick setup of simulations. It

offers a robust set of tools. Thus, it is a very useful program.

FEMM is a good program for performing easy-to-setup machining simulations. Although there are still some bugs those needs to be worked out, the program is still very functional and it is very valuable.

5. CONCLUSIONS

A geometric model of RF-PMSM suitable for EV has been presented in this work. Then this model is validated by the FEM using two softwares OPERA and FEMM. The FE study has allowed to validate the analytical calculation and to validate waveforms as well as the electromagnetic motor torque. In addition the values of flux, cogging torque curve and back-EMF found by OPERA and FEMM is almost the same. Reducing cogging torque of PMSM which cause torque pulsations and non-sinusoidal back-EMF is the theme of future research.

REFERENCES

[1] Xiang dong Liu, Hao Chen, Jing Zhao, and Anouar Belahcen, "Research on the Performances and Parameters of Interior PMSM Used for Electric Vehicles," *IEEE Transactions on Industrial Electronics, Vol 63,pp 3533-3545*, February 2016.

[2] M. Gulec , E. Yolac An, Y. Demiro , G. Ocak and M. Aydin "Modeling based on 3D finite element analysis and experimental study of a 24-slot 8-pole axial-flux permanent magnet synchronous motor for no cogging torque and sinusoidal back-EMF," *Turkish Journal of Electrical Engineering & Computer Sciences*, pp. 262–275,vol 24, January 2016.

[3] M.Chaieb "Conception, modélisation et optimisation de la motorisation d'un véhicule électrique," Ph.D. dissertation, Dept. Electrical. Engineering., Univ. Sfax, Tunisia, National Engineering School of Sfax, 2011.

[4] S. Tounsi, N. Ben Hadj, R. Neji and F. Sellami "Optimization of Electric Motor Design Parameters Maximizing the autonomy of electric vehicles," *International Review of Electrical Engineering, Vol. 2, p118* January 2007.

[5] N. Ben hadj "Amelioration des perfermances des véhicules électriques," Ph.D. dissertation, Dept. Electrical. Engineering, Univ. Sfax, Tunisia, National Engineering School of Sfax, 2011.

[6] Lingling Wang, Xin Wang , Yihui Zheng , Lixue Li , Wei Wang and Hao Wo "Finite Element Analysis of Permanent Magnet Synchronous Motor of Electric Vehicle," in Zhuhai China 2015 *icaees-15 International Conference on Advances in Energy and Environmental Science* , pp 1127-1130.

[7] E. Muljadi and J. Green "Cogging Torque Reduction in a Permanent Magnet Wind Turbine Generator," presented at the 21st American Society of Mechanical Engineers Wind Energy Symposium Reno, Nevada, January 2002

[8] Opera-2d 11.0 User Guide by Vector Fields Limited, England.

[9] Jayasankar .K.C, Dr. Rajashekhara, "Improving the Performance of PM Wind Turbine Generator by Minimizing the Detent Torque Using Finite Element Method," *International Journal of Science, Engineering and Technology Research,* Vol 2, pp 445-448, February 2013.

[10] S. Jamali Arand, M. Ardebili, "Cogging torque reduction in axial-flux permanent magnet wind generators with yokeless and segmented armature by radially segmented and peripherally shifted magnet pieces, " *Renewable Energy*, vol. 99, pp 95-106, December 2016.